A. Uhl and P. Wild. Personal identification using Eigenfeet, Ballprint and Foot geometry biometrics. In *Proceedings of the IEEE 1st International Conference on Biometrics: Theory, Applications, and Systems (BTAS'07)*, 6 pages, Washington, DC, USA, September 2729, 2007. © IEEE. http://dx.doi.org/10.1109/BTAS.2007.4401924. The original publication is available at http://www.ieeexplore.com.

Personal identification using Eigenfeet, Ballprint and Foot geometry biometrics

Andreas Uhl and Peter Wild

***Abstract*— This paper presents a new approach for personal identification using foot-biometric features based on Eigenfeet, local ridge characteristics and shape geometry. Due to the immutability of personal biometric features questions regarding privacy issues arise, when e.g. fingerprints are compromised. For niche applications, employing footprint-based authentication might bear enough security without the drawback of relying on sensitive data demanded by high-security applications. Part one of this paper outlines origins, fields of application and proposed system setup. After an introduction to employed normalization and feature extraction steps we discuss specific characteristics of foot biometrics compared to traditional hand and face-based techniques. Experimental results of all three employed biometric matchers are given and analyzed in part two. Finally, we present a summary of observed results.**

I. INTRODUCTION

Recognizing people is fundamental to many daily actions within our society and biometric research is growing rapidly. However, while common physiological biometrics used in access control systems rely on face, fingerprint, hand geometry and iris features [1], [2], foot biometry is still in the early stages of research. Starting with forensic applications by Kennedy [3] using inked barefoot impressions to extract 38 local geometrical features, there has been ongoing work in foot biometrics. A scheme operating on pressure distribution data of 10 male feet using simple Euclidian distance between footprints was introduced by Nakajima et al. [4] achieving recognition rates of 85%. More recent work concentrates on static foot shape and body posture [5] (97.8% recognition rate examining 5 subjects) and dynamic footprint-based recognition using Hidden Markov Models [6] (80% correctly classified samples of 11 subjects). Clearly, commercial applications demand higher accuracy and prospective results for larger population.

We try to improve existing recognition rates comparing three foot-biometric features which can be acquired from greyscale foot images alone, namely:

- *Eigenfeet features* (corresponding to *Eigenfaces* [7] in traditional face recognition) in the principal component subspace for recognition of both shape and textural information;
- *minutiae-based ballprint* features employing different techniques used in fingerprint verification systems; and
- *geometrical information* focusing on characteristics such as local foot widths.

A. Uhl and P. Wild are with the Department of Computer Sciences, University of Salzburg, A-5020 Salzburg, Austria {uhl,pwild}@cosy.sbg.ac.at

The application of traditional shape and skin texture biometric measurements of the human hand (such as [8], [9]) to counterparts in foot biometrics is considered complicated due to (a) close-fitting toes, (b) absence of typical expressive lines in footprints and (c) noisy creases in rotated footprints.

Tradeoffs between accuracy and human-friendliness are crucial for the design of biometric systems and it is clear, that footprint-based identification is obviously not a useful alternative in many cases (because of e.g. non-habituated environment, user-unfriendly data acquisition or uncomfortable associations at the acquisition step). But personal recognition using feet might be the biometric identifier of choice when three conditions hold:

- the environment guarantees the clean and comfortable capture of footprints,
- no high security is demanded, and
- users claim for non-invasive identifiers in the sense of privacy issues.

If these prerequisites are met, foot biometry might even be implemented as a covert system in contrast to hand biometric techniques. Due to the practice of wearing shoes in daily actions it is difficult to capture or publicly acquire footprints for attacks. Finally, precisely because foot biometry is not and probably will never be a suitable authentication mechanism for high security applications, storage of foot biometric features does not necessarily imply security threats. To improve the human-friendliness of our proposed method we have avoided pegs [10] and special illumination and extract biometric measurements out of a simple capture of the right foot by a flatbed scanning device. Potential fields of applications comprise access control in public baths, spas and also Japanese apartments [4], i.e. areas where users are not expected to wear shoes. For systems preventing unpaid admission to fee-paid areas, image capture could be executed in front of barriers (possibly underwater) supporting both prepaid (charge in advance) and pay-per-entry schemes (payment ex post by e.g. direct debit). All these examples are ideally implemented as *positive* identification schemes, i.e. determining membership by biometric features only.

The first part of this paper starts with an architectural overview in Section II and an introduction to various normalization and image enhancement steps in Section III. Section IV presents implemented biometric measurements, feature extraction and matching criteria in detail. Experimental setup and test results are presented in Section V. Finally, Section VI forms the conclusion.

II. SYSTEM ARCHITECTURE

We introduce a novel footprint-based biometric authentication system operating in *identification* mode extracting features out of *plantar*[1] foot-images alone. While *verification* systems need identifiers such as user IDs or cards in addition to biometric features and work in 1:1 comparison mode, *identification* systems are based on biometric measurements only and search the entire database for matches. For access control in spas we believe this setup to be more practical being independent of physical possessions.

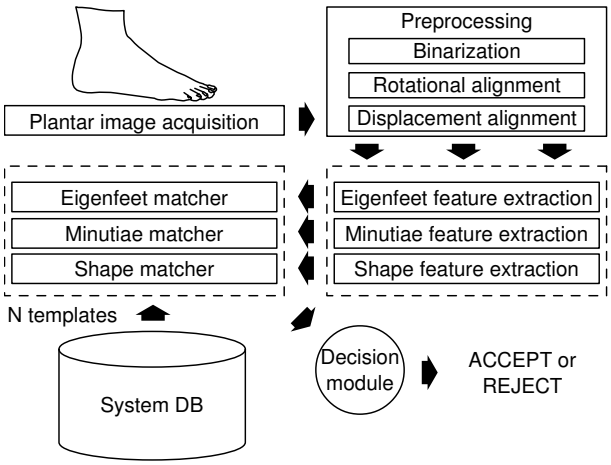

Fig. 1. Architecture of the footprint identification system

A. Proposed system

The system's architecture as depicted in Fig. 1 relies on three different techniques adopted from fingerprint verification [11], face recognition [7] and hand geometry [8] and consists of the following modules:

- **Image acquisition**: Images are captured by flatbed scanners or cameras (comparable with techniques used in *palmar*[2] hand biometric systems [9], [8]) at 600 dpi resolution.
- **Preprocessing**: The ability to normalize different rotations of feet is at the heart of the problem of preprocessing footprints and can increase recognition accuracy enormously [4].
- **Matching and Decision module**: We analyze three different matchers regarding False Acceptance Rate (FAR) and False Rejection Rate (FRR) for the positive identification task. Further extension to a *multimodal* foot biometric system [12] might be useful or even necessary since scalability issues of hand geometry (features are known to be not very distinctive and can hardly be scaled up for identification out of large population databases [1]) are most likely to be inherited to foot biometrics.

[1]**plantar** (*anat.*): towards the lower surface of the foot, i.e. sole
[2]**palmar** (*anat.*): towards the palm of the hand

III. IMAGE ACQUISITION AND ALIGNMENT

In order to separate foot texture from background (background pixels are masqueraded), *binarization* using Canny edge detection [13] with binary thresholding on the original image B is applied yielding image B_1. While using Otsu's Method has proven to be a good alternative for hand geometry [8], we have decided to use a more elaborate approach in order to reliably detect foot contours needed for shape-based feature extraction. Within the obtained image B_1 we fill the interior of the foot using binary thresholding on B, i.e. $B_2(x,y) = max(bin_b(B)(x,y), B_1(x,y))$ where $bin_b(B)$ denotes the binarization of B using threshold b. Now, this binarized image B_2 is subjected to morphological dilation using a square structuring element S to close the boundary:

$$B_3 = B_2 \oplus S = \{(x,y)|S_{xy} \cap B_2 \neq \emptyset\} \quad (1)$$

where S_{xy} denotes a shift of S by (x,y). This operation is followed by a removal of small white BLOBs and a filling of all black BLOBs except the background to get the binarized image B_4. Finally we employ morphological erosion on this image:

$$B_5 = B_4 \otimes S = \{(x,y)|S_{xy} \subseteq B_4\} \quad (2)$$

A. Rotational alignment

Rotational alignment is achieved matching footprints with the best-fitting ellipse, as described in [14]. The goal is to estimate the angle Θ between y-axis and the major axis of the best matching ellipse. Having a binary image B of size $n \times m$ and let A be the number of white pixels representing the foot, then the center of mass $C = (\overline{x}, \overline{y})$ can be determined as follows:

$$\overline{x} = \frac{1}{A}\sum_{i=1}^{n}\sum_{j=1}^{m} jB(i,j), \quad \overline{y} = \frac{1}{A}\sum_{i=1}^{n}\sum_{j=1}^{m} iB(i,j). \quad (3)$$

C is also the center of the ellipse, thus if $x' = x - \overline{x}$ and $y' = y - \overline{y}$ then the angle of inclination is given by:

$$\Theta = \frac{1}{2}\arctan\left(\frac{2\mu_{1,1}}{\mu_{2,0} - \mu_{0,2}}\right) \quad (4)$$

$$\mu_{2,0} = \sum_{i=1}^{n}\sum_{j=1}^{m}(x'_{ij})^2 B(i,j) \quad (5)$$

$$\mu_{1,1} = \sum_{i=1}^{n}\sum_{j=1}^{m} x'_{ij}y'_{ij}B(i,j) \quad (6)$$

$$\mu_{0,2} = \sum_{i=1}^{n}\sum_{j=1}^{m}(y'_{ij})^2 B(i,j) \quad (7)$$

We also consider possible holes in the image, e.g. between toes, since they have not significant influence on the result. After rotational alignment, *displacement alignment* restricts images to the bounding box containing the section of interest.

B. Adapting resolution to employed matchers

To provide each matcher with appropriate input, processed footprints are scaled to specific resolutions, i.e.

- 512×1024 for the Shape feature,

- a low 128×256 variant for Eigenfeet and
- the full 600 dpi resolution for the extraction of ridge characteristics.

The capture of highly resolved input may constitute problems when users are expected not to move during the acquisition step. For this reason we encourage the application of scanning methods supporting localized high resolution (i.e. for the ballprint region) or camera-based image acquisition to suppress noise caused by motion blur.

IV. IMAGE ACQUISITION AND ALIGNMENT

Using normalized footprint data we extract both shape and texture information by means of three different features. The first matcher uses principal component analysis on raw normalized footprint images. Similar to Eigenfaces suggested by Turk and Pentland [7] for face recognition this Eigenfeet matcher is sensitive to both geometrical and textural properties. For a probe set of 1195 facial images of subjects taken at the same time Delac et al [15] could verify PCA-based recognition rates of 82.26% at rank one, i.e. within the top one match. We expect similar reasonable identification performance for footprint images.

Typical ridge structure is also present in footprints at high resolutions even if no special ridge extraction devices such as fingerprint scanners are used. For this reason, we incorporate a minutiae based feature extraction step developed for fingerprint matching [11] estimating local ridge structure on a specified part of the footprint. Fingerprint identification has long tradition since fingerprint individuality and permanence has been widely accepted based on manual inspection of millions of fingerprints [2]. Current systems are shown to outperform face or hand-based identification techniques [16]. However, it is not yet clear if this also holds for ridge structures on footprints.

Finally, we also incorporate a geometry-based feature which takes into account that feet are characterized by their local shape characteristics. Similar to traditional hand geometrical approaches [8] examining lengths and widths of fingers we extract average local foot widths at different positions. Considering the sole of the foot to be prone to injuries shape-based features are thus expected to show constant performance also for larger time lapses between recordings. However, a problem mentioned in [4] is the fact that feet are generally about 5 mm larger in the evening than in the morning due to hypostatic congestion. Also a significant change in weight may cause high inter-personal variability.

Finally, for each algorithm a discrete matching score $m_i \in \mathbb{N} \cap [0, 100]$ for $1 \leq i \leq 6$ is calculated.

A list of implemented features for the footprint-based identification task can be found in Table I.

TABLE I
IMPLEMENTED FEATURES

Algorithm	Features	Classifier
Eigenfeet	projection of subsampled footprint onto feature space spanned by 20 most significant principal components	based on Manhattan distance
Minutiae	using the NIST [11] `mindtct` minutiae extractor on ballprint region under big toe	based on NIST [11] `bozorth` matcher
Shape	15 local foot widths and positions	based on Manhattan distance

A. Eigenfeet

The motivation behind the Eigenfeet feature, based on PCA is a classification using the most relevant features instead of an arbitrary selection of features. The main idea is to think of an image Γ as a $m \times n$ -dimensional vector which can be represented exactly in terms of a linear combination of principal components, i.e. eigenvectors (also called *Eigenfaces* for facial images), computed on the covariance matrix of training images. Eigenvectors are ordered according to eigenvalues and only the ones with the M highest eigenvalues are kept, leaving the most important features that are critical for the recognition task. Feature extraction using the Eigenfeet algorithm is equal to projecting the 128×256 input image onto the *feet space* spanned by the 20 most significant eigenvectors depicted in Fig. 2(a) obtained by a set of also 20 training images. Thus, in the strict sense the Eigenfeet feature is a both texture-based and shape-based approach since feet silhouette information is also encoded within eigenvectors.

A computation of Eigenfeet, which precedes enrollment and matching, involves the following two tasks [7]:

1) **Acquisition** of an initial training set of centered $m \times n$ foot images represented as vectors Γ_i for $i \in \{1, \ldots, M\}$ from which the average foot vector Ψ is subtracted:

$$\Phi_i = \Gamma_i - \Psi, \qquad \Psi = \frac{1}{M} \sum_{i=1}^{M} \Gamma_i \tag{8}$$

2) **Computation** of $mn \times mn$ covariance matrix:

$$\mathbf{C} = \frac{1}{M} \sum_{i=1}^{M} \Phi_i \Phi_i^T = \mathbf{A}\mathbf{A}^T \tag{9}$$

and eigenvectors u_k with according eigenvalues λ_k. For computational efficiency often the $M \times M$ Matrix $\mathbf{A}^T\mathbf{A}$ is used instead, since the M eigenvectors v_k of $\mathbf{A}^T\mathbf{A}$ correspond to the M largest eigenvalues u_k of $\mathbf{A}\mathbf{A}^T$ fulfilling the equation $u_k = \mathbf{A}v_k$ and usually M is much smaller than mn.

3) **Ordering and selection** of L highest eigenvectors with corresponding eigenvalues.

Having selected a set of Eigenfeet u_i with $i \in \{1, \ldots, L\}$ and average foot Ψ, feature extraction comprises the following steps:

1) **Normalization** of the foot vector Γ calculating $\Phi = \Gamma - \Psi$.
2) **Projection** onto eigenspace to get the feature vector components $\omega_i = u_i^T \Phi$. The feature vector consists of

(a) Eigenfeet: Computed Eigenfeet of 20 footprints

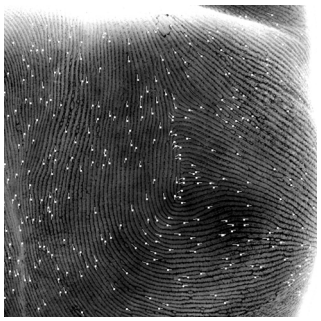

(b) Minutiae: Ballprint region containing 352 minutiae

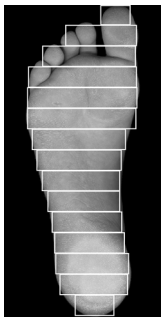

(c) Shape: Average widths of slices

Fig. 2. Visualizing Shape, Eigenfeet and Minutiae feature extraction

exactly L components $f_1 = (\omega_1, \ldots, \omega_L)$ such that Φ is approximated by:

$$\Phi \sim \sum_{i=1}^{L} \omega_i u_i \tag{10}$$

Finally, matching involves a simple distance metric in feet space with thresholding.

B. Minutiae extraction

We use the NFIS2 [11] minutiae extraction and matching software `mindtct` and `bozorth3` to extract minutiae information out of the ballprint region under the big toe. After rotational alignment we extract a rectangular region of fixed size $\frac{h}{6} \times \frac{w}{2}$ centered at $B = (\frac{3w}{4}, \frac{3h}{12})$ where h and w are the height and width of a bounding box circumscribing the input footprint. We then employ contrast improving histogram stretching on the extracted region, which is still at 600 dpi resolution. While `mindtct` binarizes this input image and detects up to 400 minutiae per ballprint image (depending on image quality, see Fig. 2(b)), `bozorth` is employed at the classification stage. A problem for highly resolved footprint images is textile defilement due to the practice of wearing socks, which was avoided in advance by cleaning the sole before image acquisition. The incorporated `bozorth3` matcher for the Minutiae feature already outputs a matching score which is used to generate a similarity score within the Minutiae matching module.

C. Shape-based feature

In order to extract shape features, the normalized footprint is divided into N vertical slices $V_0, \ldots V_{N-1}$ with equal dimensions. The y-monotone polygon S_y is now used to compute the average width of the foot per slice, i.e. the average width w_i of the set $V_i \cap S_y$ for $i \in \{0, \ldots, N-1\}$ of in-foot pixels. Using a binary representation B of size $n \times m$ and the characteristic function χ we get:

$$w_i = \frac{N}{n} \sum_{j=1}^{n} \sum_{k=1}^{m} \chi_{V_i \cap S_y}(j,k) \tag{11}$$

The final feature vector is now constructed as $f_3 = (w_2, \ldots w_{N-1})$ with $N = 15$. We neglect the first two slices to suppress noise caused by toes. A dissimilarity value is calculated in matching stage using Manhattan distance.

V. EXPERIMENTS

There are a number of errors made by biometric systems, which need to be understood and estimated before a particular biometric is selected for application. Since various error types depend on the formulation of hypotheses we explicitly refer to positive identification. Let $\mathbf{M}$ denote the database containing $m = |\mathbf{M}|$ enrolled members, then for a biometric sample f we formulate the following (null and alternate) hypotheses for the authentication task:

- H_0: there exists a member template $\exists t \in \mathbf{M}$ with a match $t \equiv f$.
- H_a: within $\mathbf{M}$ no match exists $\forall t \in \mathbf{M} : t \not\equiv f$.

Within this context, a *False Accept* occurs, if f is found to be matched with a template within $\mathbf{M}$ while in reality it is an imposter and *False Rejects* denote falsely rejected genuine authentication attempts. Matching with multiple (correct or incorrect) candidates is ignored in this case. Different algorithms are compared using FAR and FRR at different thresholds t depicted in the form of a Receiver Operating Characteristics (ROC) Curve in Fig. 4(b). Further classification of common identification systems according to [2] regarding operation mode comprise:

- **threshold-based** systems: returning a list of all database members exceeding a score $s(f, t_i)$ for each template $t_i, i = 1, \ldots, m$;
- **rank-based** systems: returning a sorted K-dimensional vector of members that best match the biometric; and
- **hybrid** approaches behaving like rank-based systems if more than K templates match (according to a defined threshold) but decrease output vector size, if less templates exceed matching scores.

Using this terminology our proposed system may be classified as a rank-based system based on scores. Therefore we also evaluate ranking behavior estimating *Rank Probability Mass* functions in Fig. 4(a). We investigate achievable recognition accuracy and both inter and intra-class variability of single incorporated foot-biometric features examining (complementary) cumulative distributions of genuine and imposter

authentication attempts diagrammed in Fig. 3. Finally, we try to analyze matching performance results.

A. Test Setup

All experiments were conducted by using our database of 135 male and 25 female footprints of 32 volunteers. We used an HP Scanjet 3500c flatbed scanning device operating at 600dpi resolution to acquire 5 footprint samples of the right foot per user. The scanner supports an area of 216 x 297 mm, which was found to be sufficient for single foot captures. Each sample as an image of 256 grey levels was recorded with the user sitting in front of the scanning device. Thus the footprints are not heavily loaded with full weight. The acquired test data set does not include any of the 20 images used for computing the predefined *Eigenfeet* matrix and only two persons are recorded in both sets. For member database enrollment we have chosen the first captured image of $m = 16$ persons yielding 64 possible genuine attempts for the remaining 4 images per user and 80 imposter attempts (each footprint was matched against the member set $\mathbf{M}$).

B. Matching Performance

Overall recognition rates for rank 1, i.e. the relative frequency of correctly identified samples based on position 1 of the ranked K-dimensional member vector, are 96.87% for Eigenfeet, 98.43% for the Minutiae algorithm and 92.19% for the Shape feature, as can be seen in Fig. 4(a). This behavior is outperforming existing footprint-based identification systems for comparable population size [4]. Inspecting the ROC-curve for the positive identification task still Minutiae based recognition shows slightly better performance than Eigenfeet (like Fingerprint recognition outperforms Face-based techniques [16]), especially for operating points with nearly equal FAR and FRR. But it should be noticed that the Eigenfeet algorithm does not need highly resolved input images and compared to other footprint-features small-sized feature vectors of 160 bytes are used. We compare operating points with closest distance to the first median with prior fusion of points sharing the same FAR or FRR rejecting the point with larger distance to the origin.

The Minutiae feature showed the best results with error rates of FAR 2.5%, FRR 3.13%. But these rates are orders of magnitude higher than reported fingerprint identification rates [16]. Possible reasons comprise a four times higher number of minutiae within the ballprint region (see Fig. 2(b)) or worn ridges especially for older users.

Also well performance could be indicated for the Eigenfeet algorithm. Its matching accuracy of FAR 2.5% and FRR 4.69% is similar to the Minutiae feature, but is not prone to textile defilement or high resolutions.

Finally the local width-based Shape feature did not produce competitive results and scalability seems to be a problem. It exhibits an FAR of 11.25% at FRR 14.06% which is significantly worse. But for fusion purposes or verification systems this technique could be a useful alternative.

Presumably, for traditional access control, where highest reliability and accessibility is required (and no privacy issues

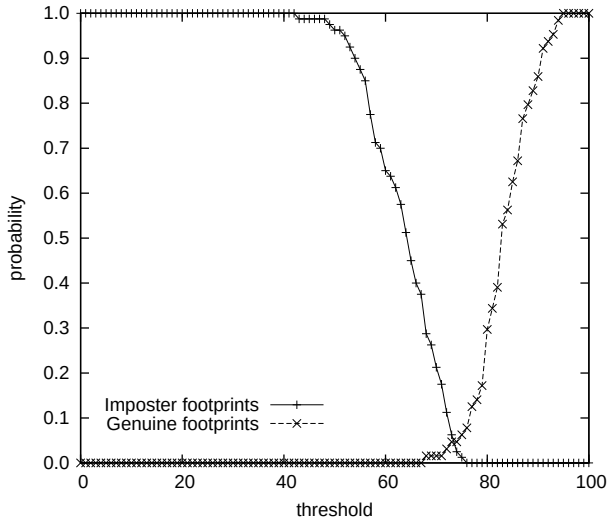

(a) Eigenfeet

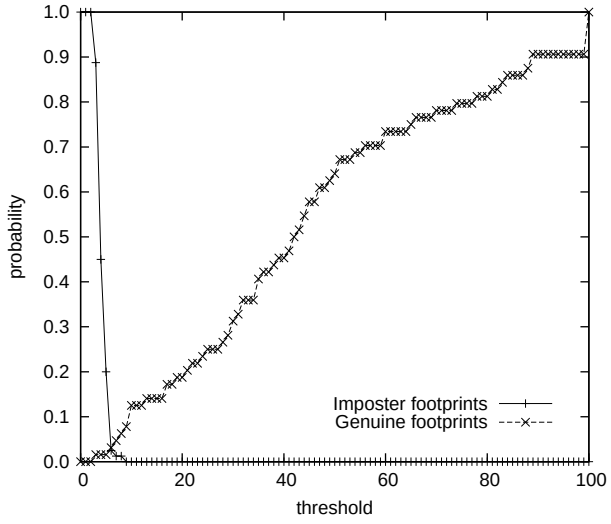

(b) Minutiae

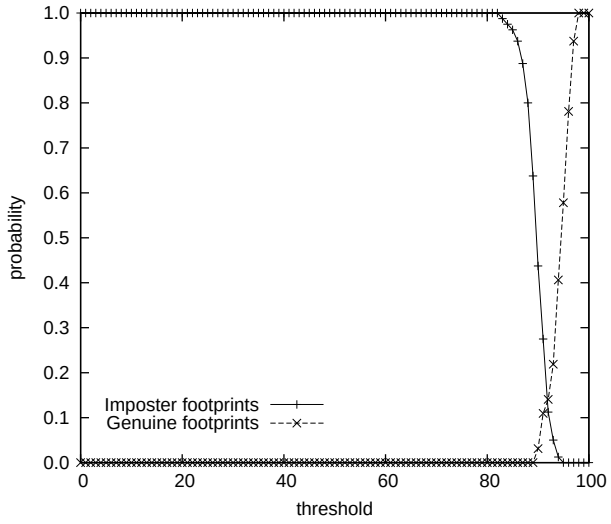

(c) Shape

Fig. 3. (Complementary) Cumulative Probability Distributions of Genuine and Imposter matching scores at rank 1

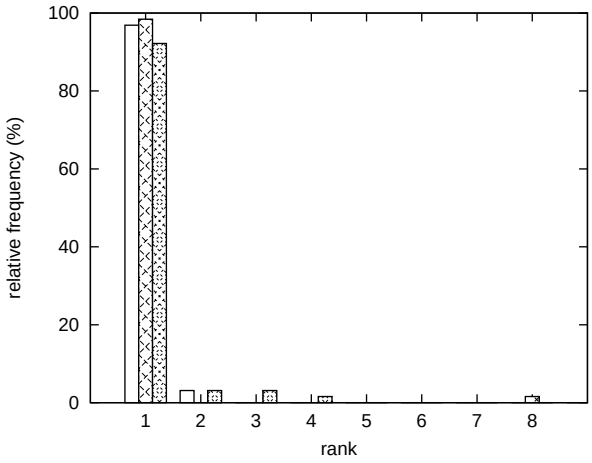

(a) Rank Probability Mass Function

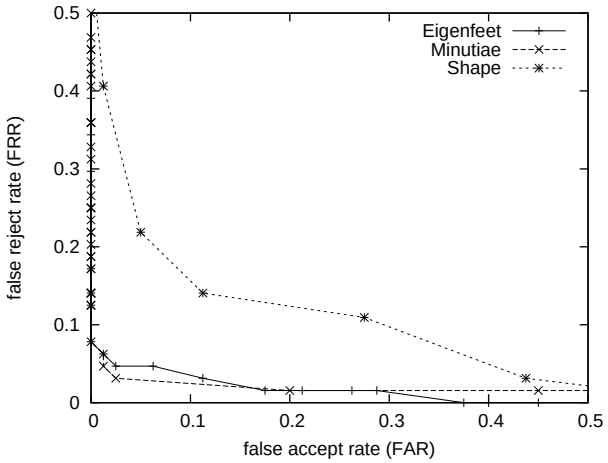

(b) Receiver Operating Characteristics

Fig. 4. Comparing footprint identification performance

TABLE II
COMPARING FAR AND FRR

Algorithm	Threshold	FAR	FRR
Eigenfeet	74	2.5%	4.69%
Minutiae	7	2.5%	3.13%
Shape	93	11.25%	14.06%

exist), it is better to stick to classical fingerprint, iris or face biometrics. But footprints could be a feature for restricted area access-control in e.g. spas or public baths, when high accessibility is achieved due to the absence of shoes and socks.

VI. SUMMARY

We have proposed a footprint-based biometric identification system employing three features, partly derived from hand, face and fingerprint biometrics [8], [7], [11] and have compared their accuracy performance.

Minutiae and Eigenfeet based upon PCA showed the best positive identification results at the operating points 2.5% FAR, 3.13% FRR and 2.5% FAR, 4.69% FRR respectively. We have experienced problems employing shape-based identification due to scalability issues yielding EERs exceeding 10% even for small database size (m =16).

The proposed approach has the advantage of being image-based and no special hardware is required to capture footprints. For future research, the effect of training set size and lime lapses between recordings on identification performance has to be examined. Additionally, different recording conditions such as wet feet (for its use in thermal baths, e.g.) deserve further attention. Combining rank-based results using fusion techniques could further improve recognition rates.

VII. ACKNOWLEDGMENTS

We would like to thank Michael Gschwandtner for the idea and source code of the Shape feature.

REFERENCES

[1] A. K. Jain, A. Ross, and S. Prabhakar, "An Introduction to Biometric Recognition," *IEEE Trans. on Circuits and Systems for Video Technology*, vol. 14, no. 1, pp. 4–20, 2004.

[2] R. M. Bolle, J. H. Connell, S. Pankanti, N. K. Ratha, and A. W. Senior, *Guide to Biometrics*. New York: Springer Verlag, 2004.

[3] R. Kennedy, "Uniqueness of bare feet and its use as a possible means of identification," *Forensic Science International*, vol. 82, no. 1, pp. 81–87, 1996.

[4] K. Nakajima, Y. Mizukami, K. Tanaka, and T. Tamura, "Footprint-based personal recognition," *IEEE Trans. on Biomedical Engineering*, vol. 47, no. 11, pp. 1534–1537, 2000.

[5] J.-W. Jung, K.-H. Park, and Z. Bien, "Unconstrained Person Recognition Method using Static and Dynamic Footprint," in *Proc. of the 18th Hungarian-Korean Seminar, Budapest, Hungary*, 2002, pp. 129–137.

[6] J.-W. Jung, T. Sato, and Z. Bien, "Dynamic Footprint-based Person Recognition Method using Hidden Markov Model and Neural Network," *Int. Journal of Intelligent Systems*, vol. 19, no. 11, pp. 1127–1141, 2004.

[7] M. Turk and A. Pentland, "Eigenfaces for Recognition." *Journal of Cognitive Neuroscience*, vol. 3, no. 1, pp. 71–86, 1991.

[8] A. Kumar, D. C. M. Wong, H. C. Shen, and A. K. Jain, "Personal Verification using Palmprint and Hand Geometry Biometric," in *Proc. of the 4th Int. Conf. on Audio-and Video-Based Biometric Person Authentication*, 2003, pp. 668–678.

[9] E. Yoruk, E. Konukoglu, B. Sankur, and J. Darbon, "Shape-based hand recognition," *IEEE Trans. on Image Processing*, vol. 15, no. 7, pp. 1803–1815, 2006.

[10] R. Sanchez-Reillo, C. Sanchez-Avila, and A. Gonzalez-Marcos, "Biometric Identification through Hand Geometry Measurements," *IEEE Trans. on Pattern Analysis and Machine Intelligence*, vol. 22, no. 10, pp. 1168–1171, 2000.

[11] "NIST Fingerprint Image Software 2," National Institute of Standards and Technology Software User's Guide, 2004. [Online]. Available: http://fingerprint.nist.gov/NFIS

[12] A. Ross and A. K. Jain, "Information fusion in biometrics," *Pattern Recognition Letters*, vol. 24, pp. 2115–2125, 2003.

[13] J. F. Canny, "A computational approach to edge detection," *IEEE Trans. on Pattern Analysis and Machine Intelligence*, vol. 8, no. 6, pp. 679 – 698, 1986.

[14] K. Sobottka and I. Pitas, "Extraction of facial regions and features using color and shape information," in *Proc. of the 13th Int. Conf. on Pattern Recognition*, 1996, pp. 421–425.

[15] K. Delac, M. Grgic, and S. Grgic, "Independent Comparative Study of PCA, ICA, and LDA on the FERET Data Set," *Int. Journal of Imaging Systems and Technology*, vol. 15, no. 5, pp. 252–260, 2005.

[16] A. K. Jain, S. Pankanti, S. Prabhakar, L. Hong, and A. Ross, "Biometrics: A Grand Challenge," in *Proc. of the 17th Int. Conf. on Pattern Recognition*, 2004, pp. 935–942.